

Effects of Refraction in Exoplanet Atmospheres on Transit Light Curves

Julia Berndtsson
julia.berndtsson@telia.com

under the direction of
Dennis Alp
Department of Physics
KTH Royal Institute of Technology

Research Academy for Young Scientists
July 12, 2017

Abstract

The interest for planets in other Solar Systems has been growing steadily since the first discovery of an exoplanet in the 90's. As new instruments are expected to be launched in the near future, the field of exoplanets becomes even more relevant due to the possibilities of new discoveries. Despite a decade of progression for refraction in exoplanet atmospheres, the phenomenon is still not widely used and should be studied further in order to promote the upcoming data. In this study, the signal strength of refraction in exoplanet atmospheres has been modeled for individual planets. The results show refraction shoulders depending on the properties of each planet. This data can be used as reference for planets with similar properties detected by the upcoming instruments. It is concluded that it is challenging to detect refraction with data from current equipment and that possibilities may appear along with the additions.

Contents

1	Introduction	1
1.1	Background	1
1.1.1	Transits	1
1.1.2	Radial Velocity Method	2
1.1.3	Transmission Spectroscopy	2
1.1.4	Refraction	3
1.2	Previous Research	3
1.2.1	Atmospheric Lensing and Out-of-Transit Spectra	3
1.2.2	Signal Strength	4
1.2.3	Clouds and Hazes	5
1.2.4	Parameters	5
1.3	Aim of Study	7
2	Method	7
2.1	Observations	7
2.2	Selection Procedure	7
2.3	Analytical Procedure	8
3	Results	9
4	Discussion	11
4.1	Signal Strength	11
4.2	Wavelengths	13
4.3	Further studies	14

1 Introduction

The upcoming year, 2018, will be a leap forward for astronomy and not least for research of planets in other solar systems, so called exoplanets. Four high precision instruments are expected to be operating in the near future: *European Extremely Large Telescope (E-ELT)*, the *Characterising Exoplanets Satellite (CHEOPS)*, the *Transiting Exoplanet Survey Satellite (TESS)* and the *James Webb Space Telescope (JWST)* [1, 2, 3, 4]. The instruments will enable further findings in this field, making it highly relevant to study the effects of refraction in exoplanet atmosphere in order to promote the upcoming data.

1.1 Background

In order to understand refraction in exoplanet atmospheres one must be familiar with methods and concepts such as the transit method, radial velocity, transmission spectroscopy and refraction.

1.1.1 Transits

Back in 1999, Charbonneau, et al., detected exoplanet HD 209458b using the transit method which uses photometric measurements to determine the flux of light. If dips in apparent brightness are seen repeatedly, it may be concluded that a planet is occulting the observed stellar disk, see Figure 1. Furthermore, the radius and period of the transiting planet can be calculated. The approximate ratio between star and planet radii can be calculated by the square root of the dip in brightness, enabling calculation of more accurate values of the planet radius if the properties of the star are known. Also, the period can easily be determined by measuring the time between each observed transit [5]. Note that the planet is treated as a perfect disk in this method, leaving the atmosphere and its possible effects out of consideration.

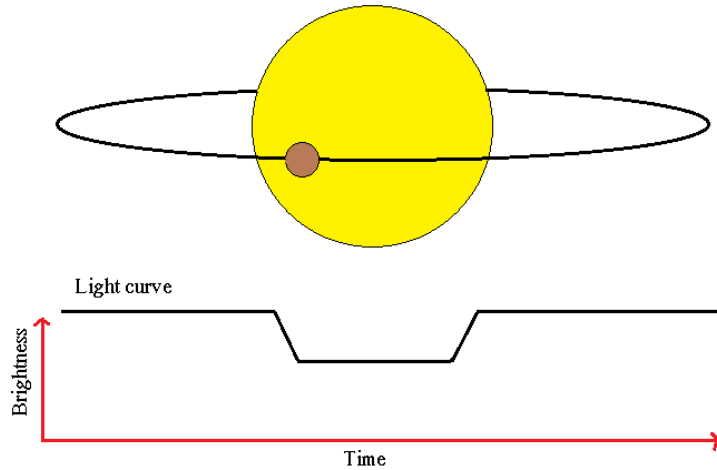


Figure 1: A planet occults a solar disk and, in turn, causes a dip in brightness as seen in the plot. In the plot, brightness can be seen on the y -axis and time on the x -axis. Note that the brightness is not to scale.

1.1.2 Radial Velocity Method

Another method for detecting exoplanets is the radial velocity method, also known as the “wobble” method [6]. A planet and its star will affect the movement of one another according to Newton’s universal law of gravitation. The planet will orbit the star due to this gravitational force and the movement of the star will be slightly affected causing it to wobble [7]. This wobble causes a measurable difference in wavelength of the light from the star, a so called Doppler shift, which can be used to determine the mass and orbital distance of the exoplanet [6, 7].

1.1.3 Transmission Spectroscopy

Transmission spectroscopy is used to deduce the composition of exoplanet atmospheres [8]. When light passes through the atmosphere of a planet, atoms and molecules will absorb certain wavelengths of the light [9]. By measuring the spectrum of this light, one can observe which wavelengths are absorbed and thereby make a comparison with the absorption spectra of known particles [9].

1.1.4 Refraction

Refraction is the phenomenon in which light changes direction when traveling through interfaces of different materials [10]. This phenomenon is rarely used in the field of exoplanets due to the imprecision of current measurements. However, it could possibly be used to reveal the composition of the inner part of the atmosphere of planets with specific properties as explained by atmospheric lensing in section 1.2.1. [11].

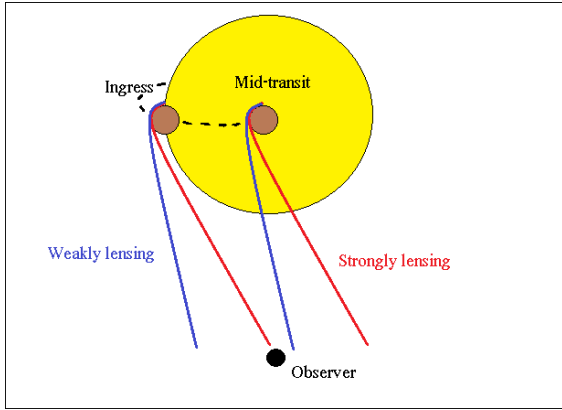
1.2 Previous Research

The field of atmospheric refraction is relatively small. However, a lot of progress has been made in the last decade resulting in the discoveries of several phenomena which were crucial in order to proceed with this study in particular.

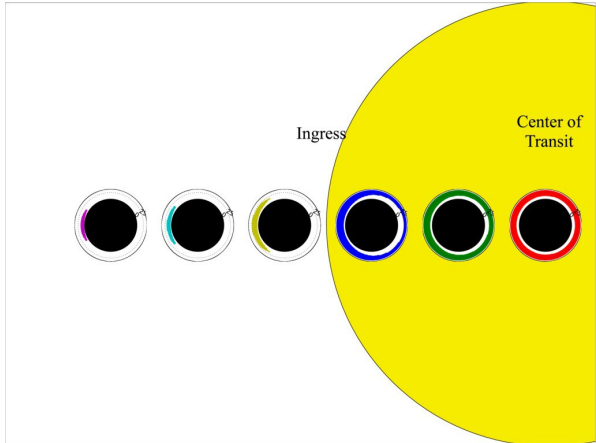
1.2.1 Atmospheric Lensing and Out-of-Transit Spectra

When light enters the atmosphere, it can refract in different angles and therefore affect what can be observed. This phenomenon is called atmospheric lensing. A planet can either be strongly lensing or weakly lensing. If strongly lensing, the light shining through the atmosphere of the planet will be refracted in a sharp angle. For a weakly lensing planet the angle will be much smaller as seen in Figure 2a. The lensing of the planet will depend upon a variety of parameters such as scale height, which could be explained as a measurement of the height of the atmosphere; radius; distance to star; and the density of the atmosphere [12]. In the case of strong lensing, one will have trouble observing the light passing through the deepest layers of the atmosphere, as seen in Figure 2b. This is due to the light being refracted out of sight [11].

There is, however, another way to observe the light passing through the region closest to the surface of the planet. Before the planet transits its star, the light may refract into line of sight, as can be seen through the illustrations in Figure 2. As a consequence,



(a) An illustration of strong and weak lensing. The red line represents the refracted light for a strongly lensing planet while the blue line represents the refracted light for a weakly lensing planet. Note that the observer cannot see the light mid-transit in the case of strong lensing.



(b) An illustration of refraction for a strongly lensing planet during ingress. The colored regions of the atmosphere shows light which can be seen by the observer and the white areas correspond to areas in which light is deflected out of sight.

Figure 2: Consequences of atmospheric lensing explained through illustrations.

a transmission spectrum of that light will reveal the composition closest to the surface of the planet [12]. In order to do so, however, the light must be detectable.

1.2.2 Signal Strength

An important factor for detection of atmospheric refraction is signal strength. Signal strength can be defined as

$$S_{\Delta t} = \Delta F / \Delta t = (F_R - F_M) / \Delta t \quad (1)$$

in which F_R is the flux detected from a normal transit and F_M is the fitted model in which refraction has been taken into consideration. At certain points, the fitted light curve will have an excess or shortage in flux in relation to the standard transit model, and the excess seen in Figure 3 can be referred to as a refraction shoulder. The signal strength can be interpreted as a measurement of how strongly refraction affects transit light curves, quantifying its detectability for a given photometric precision. [12]

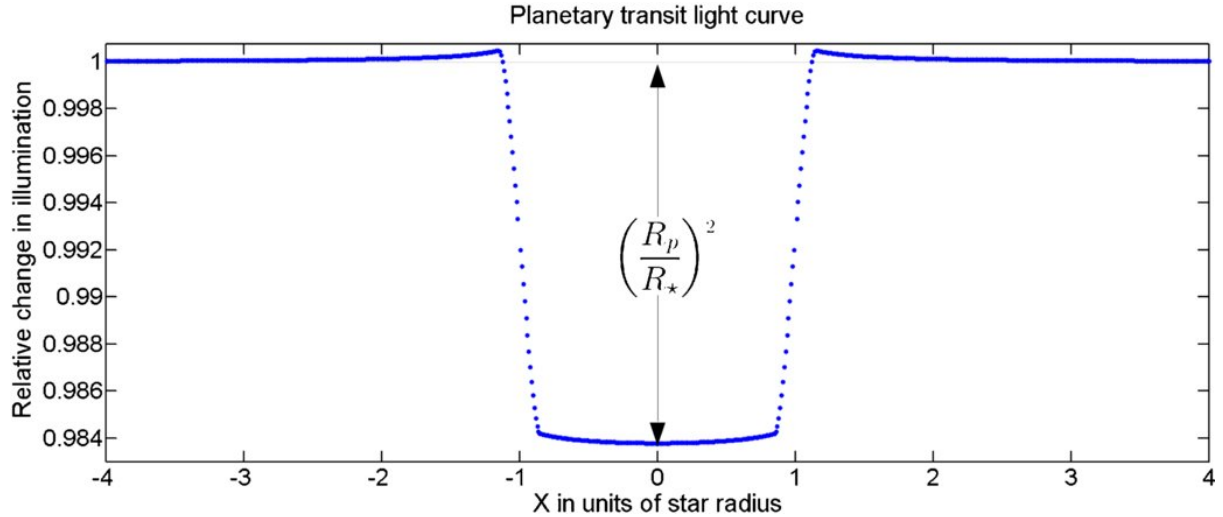


Figure 3: A transit light curve in which atmospheric lensing is considered, plotting relative change in brightness, i.e. difference in flux, on the y-axis against the planet-star distance of the planetary transit on the x-axis. The value $y = 1$ can be interpreted as the baseline of the flux of the star. Note that the light curve slightly increases when entering and exiting occultation at $x = -1$ and $x = 1$. This increase is referred to as a refraction shoulder and is caused by atmospheric lensing.

1.2.3 Clouds and Hazes

Misra, et al., (2014) concluded that clouds and hazes would affect refraction signals and transmission spectra. If light refracts through the atmosphere without encountering any haze or clouds it will result in a stronger signal [11]. In turn, one may conclude that a planet with weaker signal than predicted likely contains clouds or hazes in its atmosphere [12]. Also, if the signal measured is consistent with expectations the opposite is true, i.e. the atmosphere is clear [11].

1.2.4 Parameters

If a planet is strongly lensing, a strong signal is desirable in order to be able to measure a transmission spectrum. The equations of Hui & Seager (2002) contained different parameters which would affect refraction [14]. Alp & Demory (2017) later used these parameters to study what values would give the strongest refraction signal and concluded that a specific combination of molecular weight, mass and inverse temperature would give the maximal signal strength for planets with set values for radius and orbital distance [12].

Other parameters of significance are effective radius, meaning the observed radius when a planet blocks out light during a transit; planet mass, scale height of the atmosphere; orbital distance; the wavelength in which refraction is observed as well as the properties of the star [12, 14]. This can be seen in the equations by Hui & Seager (2002). A correlation between the scale height of the atmosphere and the temperature and composition of the planet can be seen in

$$H = \frac{k_B T}{g \mu m_H}, \quad (2)$$

where H is the scale height of the atmosphere, k_B is the Boltzmann constant, T is temperature, g is surface gravity, μ is mean molecular weight, and m_H is hydrogen atomic mass. Define B as

$$B \equiv 2\alpha \frac{\rho_0}{H} \frac{D_{LS} D_{OL}}{D_{OL} + D_{LS}} \approx 2\alpha \frac{\rho_0}{H} D_{LS}, \quad (3)$$

where α is the refractive coefficient, ρ_0 is the atmospheric density at the effective radius, D_{LS} is the distance between the planet and the star and D_{OL} is the distance between the planet and the observer. Define C as

$$C \equiv R_0/H, \quad (4)$$

where R_0 is the effective radius. According to Hui & Seager, Eq. (4) represents the binding energy to thermal energy and Eq. (3) a deflection angle scaled by ratio of distances [14].

Using these three equations, a fourth one can be derived describing whether a planet, which is assumed to be spherical, is strongly lensing if the following condition is fulfilled

$$1 - \sqrt{\frac{\pi}{2C}} B < 0. \quad (5)$$

Despite having these models formulated in theory, they are yet to be put into practice.

1.3 Aim of Study

The aim of this study was to examine the signal strength of individual planets using the models of Alp & Demory. The proposed question is: what signal strength can be expected and is it detectable in current data or with future observations?

2 Method

This study is based upon the papers by Hui & Seager (2002) and Alp & Demory (2017). There was a selection procedure, in which suitable planets were chosen, and an analytical procedure, predicting the signal strength of those planets.

2.1 Observations

The data used in this study came from *Kepler*. The data were downloaded from NASA on 23 January 2017¹ and objects which were unlikely to be planets were removed. The remaining data were fitted using a model by Mandel & Agol (2002) in order to go through several fitting and filtering procedures as described by Alp & Demory (2017). This resulted in 2394 fitted light curves, each one representing a potential exoplanet, out of the initial 4707 detected objects. [12]

2.2 Selection Procedure

In the first step, a Python script was used to visualize and manage the fitted data. A filter taking radius, photometric precision, and orbital distance into consideration was then applied using the same script. For radii, the filter demanded a radius of $0.05 R_{\odot} < R_0 < 0.3 R_{\odot}$ (R_{\odot} = solar radii). The lower limit was set to $0.05 R_{\odot}$ as planets with strong signal strength usually are similar in size to Jupiter, which has a radius of about $0.1 R_{\odot}$. As for the upper limit, an object with $R_0 > 0.3 R_{\odot}$ was considered unlikely to be a planet as it is too large. The orbital distance had to be $> 7.5 R_{\odot}$ as this affected the error as well as

¹<http://exoplanetarchive.ipac.caltech.edu>

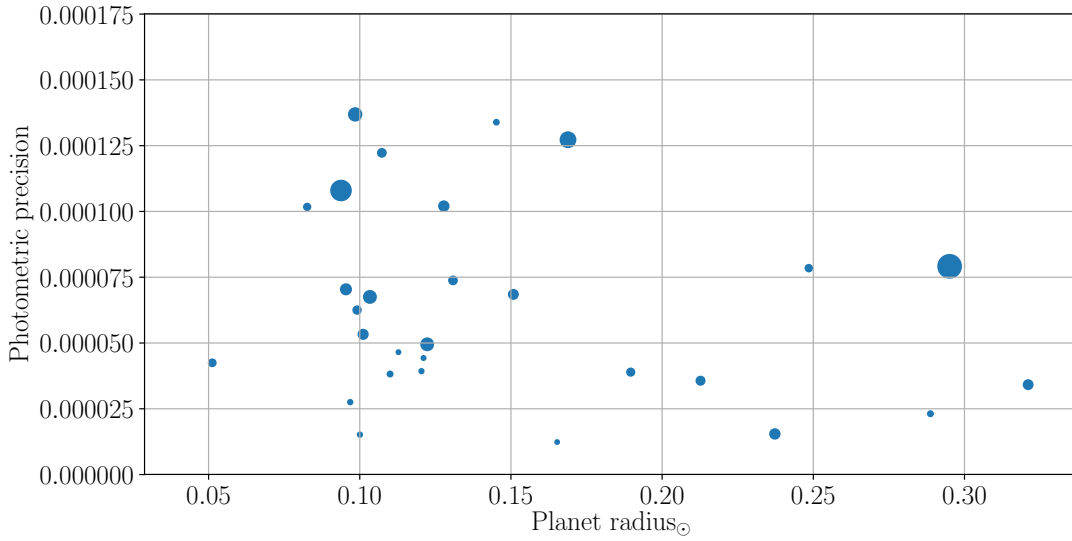


Figure 4: A graph plotting radius, accuracy and orbital distance of exoplanets in the selection procedure. The accuracy can be found on the y -axis, planet radius on the x -axis and the orbital distance is seen as the size of the data point in which a larger point represents a larger orbital distance.

the likelihood of the refraction shoulders being observable in red light.

When selecting what planets to analyze further, the graph in Figure 4 was used. Candidates with a high accuracy and large planet radius were then checked against the NASA exoplanet archive [15]. Unless the object was labeled as a false positive, i.e. confirmed as a non-planet, it was used in the next procedure.

2.3 Analytical Procedure

The objects were analyzed using a Python script to plot the expected signal strength. The script plotted signal strength from the model by Alp & Demory based upon the equations by Hui & Seager mentioned in section 1.2.4. The plotted graphs showed the refraction shoulders depending on the parameters wavelength, star radius, star mass, temperature of atmosphere, mean molecular weight, atmospheric composition, mass of planet, planet radius, and orbital distance, respectively. Several graphs were then created for varying wavelengths, temperatures, compositions, and masses in order to achieve a

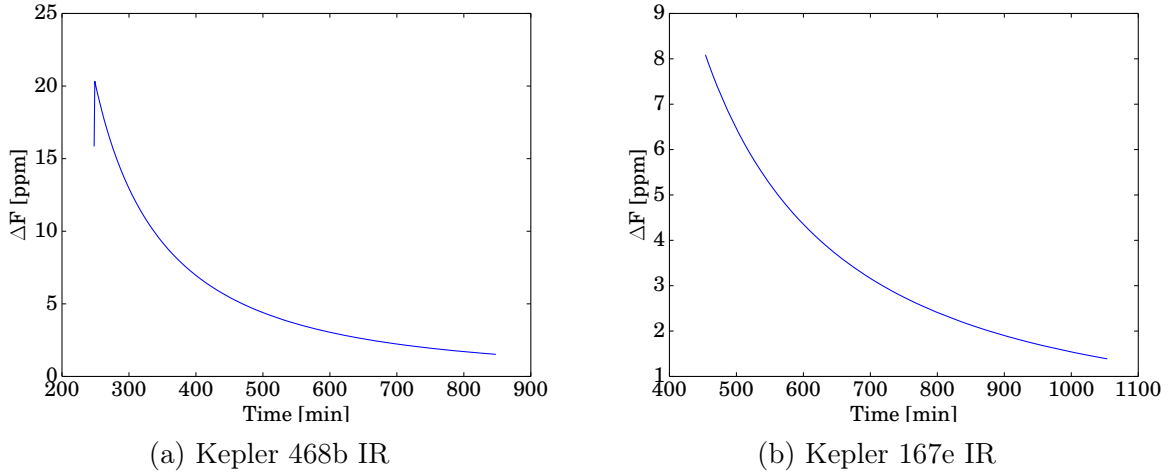


Figure 5: The refraction shoulders of planets Kepler 468b and Kepler 167e in infrared. The difference in flux in ppm can be found on the y -axis and the time after mid-occultation can be found on the x -axis in minutes.

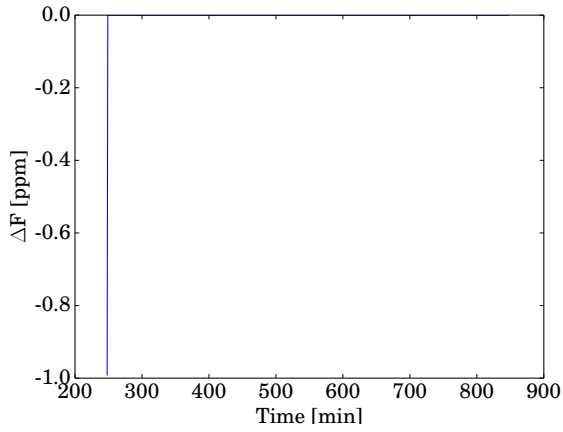
Table 1: Values of the properties used for modelling the signal strength of each respective planet.

Planet	Mass [g]	Radius [cm]	Temp [K]	Orbital distance [AU]	Period [days]
Kepler 167e	$1.28 \times 1.898 \times 10^{30}$	8.98×10^9	129	1.90	1071.2
Kepler 468b	$1.22 \times 1.898 \times 10^{30}$	8.54×10^9	484	0.48	38.5
Kepler 485b	$1.24 \times 1.898 \times 10^{30}$	8.68×10^9	1243	0.042	3.2
KOI 5708.01	$1.35 \times 1.898 \times 10^{30}$	2.03×10^{10}	1057	0.12	7.8

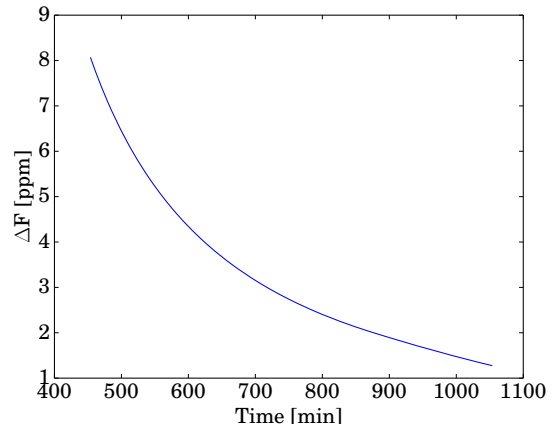
strong signal strength. Values for star mass and radius, planet radius, and orbital distance were gathered from the earlier mentioned fitted data.

3 Results

The graphs in Figures 5–7 show some of the results from this study. Each graph plots ΔF in ppm on the y -axis and time in min on the x -axis. The value of ΔF is the difference in flux and time refers to the time before the planet enters occultation, see Eq. (2). The graphs are marked IR and R, meaning infrared or red wavelength, $4.5 \mu\text{m}$ and 6500 \AA , respectively.

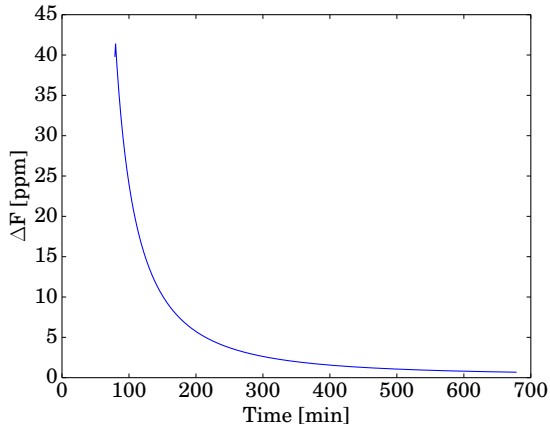


(a) Kepler 468b R

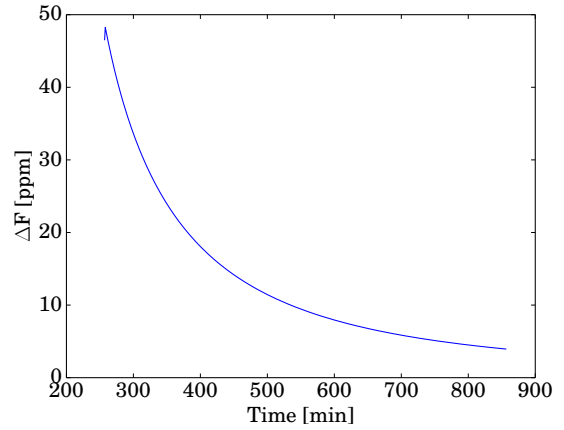


(b) Kepler 167e R

Figure 6: The refraction shoulders of planets Kepler 468b and Kepler 167e in red light. The difference in flux in ppm can be found on the y -axis and the time before occultation can be found on the x -axis in minutes. In graph (a) Kepler 468b can be seen having a signal strength of 0 ppm as it is weakly lensing.



(a) Kepler 485b IR



(b) KOI 5708.01 IR

Figure 7: The refraction shoulders of planets Kepler 485b and KOI 5708.01 in infrared. The difference in flux in ppm can be found on the y -axis and the time before occultation can be found on the x -axis in minutes.

Table 2: The peak amplitude, half-time and photometric precision of each plotted graph. Half-time is defined as the time from peak amplitude to half peak amplitude.

Planet	Wavelength [IR/R]	Peak amplitude [ppm]	Half-time [min]	Photometric precision
Kepler 167e	IR	8	175	-
Kepler 468b	IR	20	40	4.95×10^{-5}
Kepler 485b	IR	41	27	4.43×10^{-5}
KOI 5708.01	IR	48	42	2.31×10^{-5}
Kepler 167e	R	8	175	-
Kepler 468b	R	0	0	4.95×10^{-5}

4 Discussion

The values for mass and composition used when modeling the graphs in Figures 5–7 were approximated based upon the properties of Jupiter as the actual compositions and masses of the modeled exoplanets are not currently known. The orbital distances and radii for Kepler 468b, Kepler 485b and KOI 5708.01 imply that they are hot gas giants, making the composition of Jupiter likely. As for Kepler 167e it has a longer orbital distance and larger radii than the others. The composition of Jupiter was still approximated due to the size of the radius of Kepler 167e being similar to a gas giant. The masses of the planets were approximated by multiplying the mass of Jupiter with the ratio between the radii of each respective planet and Jupiter.

4.1 Signal Strength

As can be seen in Figure 5, Kepler 167b has a weaker signal than Kepler 468b, despite having a similar mass, radius and composition. This can be seen in Tables 1 and 2. However, the planets have rather different orbital distances. Kepler 167b is 1.9 AU from its star and Kepler 468b 0.48 AU. Thus, the orbital distance is to likely be one of the significant factors for the difference in signal strength. Notice that the signal can be stronger for planets with shorter orbital distances. This is a result of the temperature of the planet increasing due to the closeness to the star, in turn, increasing the scale height in Eq. (2). Also, more transits will have been observed for a shorter orbital distance in the same amount of time due to the period being shorter. This results in better accuracy of the data and, as a consequence, increases the signal-to-noise ratio, which benefits the detectability. It is not obvious, however, that this should be the case as a longer orbital distance would result in the light refracting in a less sharp angle than for a planet with a short orbital distance, in turn causing the refracted light to be more easily detectable [12].

In Figure 7, a number of parameters result in the different signal strengths for both

planets. It can be noticed that Kepler 485b has a much shorter orbital distance than KOI 5708.01, as seen in Table 1. In contrast to the earlier statement that a shorter orbital distance results in a stronger signal strength, the graphs in Figure 7 show a stronger refraction signal for KOI 5708.01 with the longer orbital distance. This is due to the masses and radii of the planets being larger and the orbital distance causing the light to refract in a less sharp angle. As pointed out by Alp & Demory, the radius is a significant factor for signal strength as it increases the projected region of refracted light, see Figure 2b. In the case of Figure 7, KOI 5708.01 has a larger radius and mass than Kepler 485b, resulting in a higher amplitude. The difference between the orbital distances of the planets was not large enough to affect the accuracy of the data significantly, resulting in KOI 5708.01 benefiting from its long orbit. Regarding the time interval for respective planet it can be concluded that the radius and orbital distance affect the ability to detect refraction. As for what time interval is beneficial when observing refraction in exoplanet atmospheres, it will depend upon several parameters that in some cases are dependent upon the telescope used for observation. The interval must be long enough for the signal to be detected but short enough for the fitted light curve F_M to be separable from the normal transit curve F_R . As a consequence, a single beneficial time interval cannot be defined but depends upon the situation.

As earlier mentioned in section 1.2.3., Misra, et. al., (2014) concluded that clouds and hazes will affect atmospheric refraction [13]. If the atmosphere is not clear, light may be obscured and as a consequence limit the signal strength. As this study predicts the signal strength for detected exoplanets with the assumption that the atmospheres are clear, the results could be used as reference values for planets with similar properties. If the measured signal of a planet does not meet its expected strength, there would likely be non-transparent clouds or hazes in its atmosphere.

Based upon these findings the following can be concluded: a long orbital distance will

give a stronger signal strength, however, the number of transits will affect the accuracy of the data; a beneficial time interval cannot be generally defined and clouds and hazes can possibly be detected using the reference values from this study.

4.2 Wavelengths

When observing exoplanets it should be noticed that the effective radii may differ due to the phenomenon Rayleigh scattering [14]. As a result, the effective planet radius will depend on the wavelength at which the planet is observed due to the ability of the light to reach different depths when refracting through the atmosphere. The scale height of the atmosphere will be affected by these different perceptions of radii, resulting in different predicted signal strengths as seen in the equations of Hui & Seager (2002). This phenomenon can be seen in Figure 5 and 6, where Figure 5 is observed in infrared light and Figure 6 in red. In Figure 6a the refraction shoulders of Kepler 468b was not observable in red light due to the planet not fulfilling the conditions for a strongly lensing planet in Eq. (5). This can be explained by the effects upon effective radii. As for Kepler 167e it can be noted that the signal strength is the same regardless of wavelength. This is due to the long orbital distance of the planet, which implies a small deflection angle.

Regarding observations, there are two telescopes with data that could potentially detect refraction in exoplanet atmospheres: *Kepler* and *Spitzer*. *Kepler* observes in red light, which is not optimal for detecting refraction due to Rayleigh scattering setting effects upon effective radius. *The Kepler Mission* aimed to detect transiting exoplanets by observing a specific area of the sky [16]. The region which the mission observes, however, is not optimal for detection of refraction in exoplanet atmospheres. The stars are too far away for detailed follow-up observations, resulting in a low observed flux and low accuracy of the data. As the data cannot be measured precisely enough, the refraction shoulders can likely not be detected.

The Spitzer Telescope detects infrared radiation, making it a suitable instrument for observing strongly lensing planets. However, *Spitzer* does not have the photometric precision to detect refraction. The mission is also based upon pointed observations of exoplanets and therefore does not observe the same regions long enough to gather the data needed to distinguish the refraction shoulders either.

To conclude, current equipment likely has not detected refraction in exoplanet atmospheres due to the data not being gathered with high enough photometric precision.

4.3 Further studies

Regarding observations, the measurements made with the upcoming high precision equipment will likely have the capacity to detect the needed differences in flux. *JWST* and *CHEOPS* are two of these instruments. There is a possibility, though, that the same issue will be faced as with *Spitzer* where the pointed telescopes will not observe the same region long enough for the needed data to be gathered. Furthermore, *TESS* aims to observe stars much brighter than the ones observed by *Kepler* [2]. As a result, the possibilities of detecting the observational flux needed in order to observe refraction shoulders are much better. *TESS* will scan a large region in order to detect exoplanets of interest, but will lack the photometric precision to detect refraction shoulders on its own. Pointed telescopes, such as *JWST* and *CHEOPS*, would thereafter be able to make more precise observations, possibly detecting refraction shoulders.

Furthermore, the model itself would be beneficial to develop in the future. Due to the complexity of the equations by Hui & Seager, a lot of computational resources is needed in order to perform the calculations. Formulating a different but more efficient model could enable faster calculations and, in turn, increase possibility of detecting refraction in exoplanet atmospheres.

Acknowledgements

First, I would like to thank my mentor Dennis Alp for these incredible weeks at KTH. They have been highly inspiring and rewarding, mostly due to his engagement. Dennis taking his time to teach us about his research has been of highest value for me and my project partner, and cannot be emphasized enough. I would also like to thank my project partner Anja Saksi for her fantastic companionship and friendship during this time and forward. Furthermore, this project would not have been possible without the amazing Rays – for excellence team and contributing partners Europaskolan and Kjell och Märta Beijers Stiftelse.

Figure References

Figure 2: Misra A, Meadows V, Crisp D. *The effects of refraction on transit transmission spectroscopy: application on Earth-like exoplanets*. The Astrophysical Journal. 2014 September 1.

Figure 3: Sidis O, Sari R. *Transits of transparent planets - Atmospheric lensing effects*. Hebrew University, Caltech. The Astrophysical Journal. 2010 September 1.

References

- [1] NASA. *About The James Web Space Telescope*. <https://www.jwst.nasa.gov>
- [2] NASA. *The TESS Mission Overview*. <https://tess.gsfc.nasa.gov/overview.html>
- [3] ESA. *Cheops Objectives*. <http://sci.esa.int/cheops/54031-objectives/>
- [4] ESO. *The European Extremely Large Telescope ("E-ELT") Project*. <https://www.eso.org/sci/facilities/eelt/>
- [5] Charbonneau D, M. Brown T, W. Latham D, Mayor M. *Detection of planetary transits across a sun-like star*. *The Astrophysical Journal*. 1999 December 16.
- [6] NASA's Jet Propulsion Laboratory. *Watching for wobble: Radial velocity*. California Institute of Technology. <https://exoplanets.nasa.gov/interactable/11/>
- [7] Wolf P, Wood E. *Extrasolar Planets*. University of Colorado at Boulder; 2007 <http://lasp.colorado.edu/education/outerplanets/exoplanets.php>
- [8] Richmond M. *Spectroscopy of exoplanets*. Rochester Institute of Technology; 2016. <http://spiff.rit.edu/classes/resceu/lectures/spectra/spectra.html>
- [9] The Editors of Encyclopedia Britannica. *Spectroscopy*. Encyclopaedia Britannica, inc; 18 January 2017. <https://www.britannica.com/science/spectroscopy/Applications#ref620112>
- [10] The Editors of Encyclopaedia Britannica. *Refraction*. Encyclopaedia Britannica, inc.; 2014 April 14. <https://www.britannica.com/science/refraction>
- [11] Misra A, Meadows V, Crisp D. *The effects of refraction on transit transmission spectroscopy: application on Earth-like exoplanets*. *The Astrophysical Journal*. 2014 September 1.
- [12] Alp D, Demory B.-O. *Refraction in exoplanet atmospheres*. KTH Royal Institute of Technology, University of Bern; 2017 (Submitted to A&A).
- [13] Misra A, Meadows V. *Discriminating between cloudy, hazy and clear sky exoplanets using refraction*. *The Astrophysical Journal*. 2014 November 1.
- [14] Hui, Seagler. *Atmospheric lensing and oblateness effects during an extrasolar planetary transit*. *The Astrophysical Journal*. 2002 June 10.
- [15] NASA. *NASA Exoplanet Archive*. https://exoplanetarchive.ipac.caltech.edu/cgi-bin/TblView/nph-tblView?app=ExoTbls&config=cumulative&constraint=koi_pdisposition+like+%27CANDIDATE%27
- [16] NASA. *Kepler Overview*. https://www.nasa.gov/mission_pages/kepler/overview/index.html